Cxcr4 regulation of interneuron migration is disrupted in 22q11.2 deletion syndrome

Daniel W. Meechan[a,b], Eric S. Tucker[c,d], Thomas M. Maynard[a,b], and Anthony-Samuel LaMantia[a,b,1]

[a]Department of Pharmacology and Physiology and [b]George Washington Institute for Neuroscience, George Washington University, Washington DC, 20037; and [c]Department of Neurobiology and Anatomy and [d]Center for Neuroscience, West Virginia University School of Medicine, Morgantown, WV 26506

Edited by Gail Mandel, Howard Hughes Medical Institute and Oregon Health and Science University, Portland, OR, and approved September 28, 2012 (received for review July 10, 2012)

Interneurons are thought to be a primary pathogenic target for several behavioral disorders that arise during development, including schizophrenia and autism. It is not known, however, whether genetic lesions associated with these diseases disrupt established molecular mechanisms of interneuron development. We found that diminished 22q11.2 gene dosage—the primary genetic lesion in 22q11.2 deletion syndrome (22q11.2 DS)—specifically compromises the distribution of early-generated parvalbumin-expressing interneurons in the *Large Deletion* (*LgDel*) 22q11.2DS mouse model. This change reflects cell-autonomous disruption of interneuron migration caused by altered expression of the cytokine C-X-C chemokine receptor type 4 (Cxcr4), an established regulator of this process. Cxcr4 is specifically reduced in *LgDel* migrating interneurons, and genetic analysis confirms that diminished *Cxcr4* alters interneuron migration in *LgDel* mice. Thus, diminished 22q11.2 gene dosage disrupts cortical circuit development by modifying a critical molecular signaling pathway via Cxcr4 that regulates cortical interneuron migration and placement.

Behavioral and psychiatric diseases, including autism and schizophrenia, are considered disorders of cortical circuitry (1–3). Despite variable onset and severity, the available evidence suggests that aberrant neural development leads to inappropriate circuit formation in these disorders. Cortical interneurons—essential regulators of cortical activity and synchrony for complex functions such as social interaction, learning, and memory (4)—are thought to be primary targets for this developmental pathogenesis (5–7). Indeed, the most consistent observations in postmortem cortex from patients with schizophrenia include altered interneuron number, distribution, or gene expression (8, 9). These studies cannot resolve whether such changes reflect developmental causes or pathologic consequences of cortical circuit dysfunction. Moreover, it is not clear whether pathogenic processes that lead to these disorders disrupt established or novel mechanisms that regulate interneuron development. Thus, we determined whether key cellular mechanisms and molecular pathways known to regulate interneuron differentiation are disrupted in the *LgDel* mouse model (10) of 22q11.2 deletion syndrome (22q11.2DS), a genetic syndrome highly associated with cortical circuit disorders.

The microdeletion at chromosome 22q11.2 that gives rise to 22q11.2DS is one of the most significant genetic risks for cortical circuit disorders (11–13). Postmortem studies of the cerebral cortex from 22q11.2DS patients implicate abnormal neuronal migration (14); imaging demonstrates related cortical anomalies including polymicrogyria and region-selective gray matter thinning (15, 16); and magnetic resonance spectroscopic studies show reduced GABA function (17). Thus, in 22q11.2DS, the available evidence indicates that cortical circuits are compromised and GABAergic interneurons are altered. We now report in the *LgDel* mouse—in which recent studies (18–20) suggest that cortical circuit assembly and function is compromised—a mechanistic relationship between diminished 22q11.2 dosage and a key molecular pathway that regulates interneuron migration during cortical development. *LgDel* interneuron phenotypes reflect interneuron-specific disruption of cytokine receptor Cxcr4, which has been shown to influence placement, migratory trajectory, and motility of these cells during cortical development (21–25). Thus, we define a relationship between 22q11.2DS, a compelling example of a copy number variant (CNV) syndrome thought to cause cortical circuit disorders, and Cxcr4-mediated signaling, an established mechanism that ensures normal cortical interneuron development.

Results

Disrupted Interneuron Placement in the *LgDel* Cortex Is Cell-Class Specific. Our previous work indicates that interneuron distribution is altered in the *LgDel* cortex, with an apparent shift of parvalbumin cells toward more superficial layers at the expense of deeper layers (18). To determine whether this defect is similar to those associated with other mutations that alter laminar distribution of interneurons (22, 26, 27), we evaluated the frequency and laminar distribution of molecularly distinct interneuron classes in the *LgDel* mouse. Among four subtypes, we found specific disruption of parvalbumin interneurons (Fig. 1 *A* and *B* and Fig. S1). These changes are reminiscent of those reported for a small number of single-gene mutations that disrupt interneuron migration and placement, including *Cxcr4* (22), *Lhx6* (26), and *Cxcr7* (27).

The laminar distribution of parvalbumin cells follows an inside–out gradient that reflects interneuron birthdates (28). To assess whether parvalbumin cell redistribution in *LgDel* mice is specific to interneurons born during particular embryonic epochs, we measured the cortical distribution of birth-dated interneuron subclasses born at embryonic day (E)13.5 and E15.5, respectively. We found that laminar redistribution is limited to E13.5-born parvalbumin cells. More of these cells are located superficially and fewer in deeper layers parallel to the overall redistribution of parvalbumin interneurons (Fig. 1*C*). Thus, interneuron placement is disrupted by diminished 22q11.2 dosage, similar to the disruption caused by single-gene mutations that compromise interneuron migration and placement.

Altered Interneuron Migration and Motility in the Embryonic *LgDel* Cortex. Changes in the distribution of cortical interneurons have been associated with genetic mutations that disrupt the migration of these cells during early development (22, 26, 27). To determine whether migration of basal forebrain-derived interneurons into the cortical rudiment is indeed altered in the *LgDel* 22q11.2DS model, we used a *Dlx5/6* Cre-IRES-eGFP (CIE) reporter mouse line that labels postmitotic neurons generated in the basal forebrain (29). We found that interneurons advance less toward the dorsal aspect of the cortex in *LgDel* than in WT E13.5 embryos (Fig. 2 *A* and *B*) similar to migration deficits in homozygous *Lhx6*-mutant embryos (30).

Author contributions: D.W.M., E.S.T., T.M.M., and A.-S.L. designed research; D.W.M. and E.S.T. performed research; T.M.M. contributed new reagents/analytic tools; D.W.M. analyzed data; and D.W.M. and A.-S.L. wrote the paper.

The authors declare no conflict of interest.

This article is a PNAS Direct Submission.

[1]To whom correspondence may be addressed. E-mail: lamantia@gwu.edu.

This article contains supporting information online at www.pnas.org/lookup/suppl/doi:10.1073/pnas.1211507109/-/DCSupplemental.

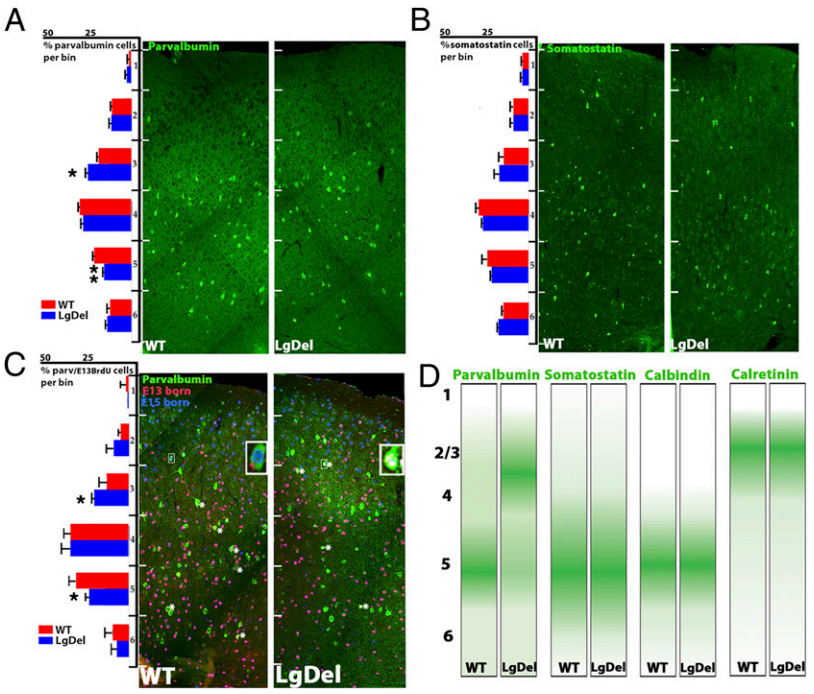

Fig. 1. The laminar distribution of early-born parvalbumin interneurons is selectively altered in the *LgDel* cortex. Counting boxes (600- μm wide and divided into equidistant bins) spanning the cortex between the pial surface and white matter tract were analyzed in coronal brain sections as described previously (18). (*A*) Parvalbumin cells are significantly redistributed (ANOVA, $n = 5$ per genotype; significant differences comparing bins between genotypes determined by LSD test, $P = 0.05$ at bin 3 and 0.0017 at bin 5; error bars represent SEM) but not for the other primarily MGE-derived interneuron subtype, somatostatin (*B*). (*C*) Parvalbumin interneurons birth-dated at E13.5 by BrdU and then at E15.5 by IdU injection, were quantified using the same sampling strategy. *Insets* show parvalbumin interneurons with E13.5 (yellow nuclei) or E15.5 (blue nuclei) birthdates. A significant redistribution of E13.5-born parvalbumin cells was observed in the *LgDel* (ANOVA, $n = 5$ per genotype, $P = 0.05$ at bin 3 and 0.048 at bin 5). Asterisks mark E13.5-born BrdU-labeled parvalbumin cells. (*D*) Schematic of interneuron distribution in P21 cortex. Interneurons that are derived mainly from the caudal ganglionic eminence or are of broad origin are not altered in frequency or distribution in the *LgDel* (see Fig. S1 for calbindin and calretinin results), unlike the parvalbumin population derived from the MGE.

To determine whether these changes reflect reduced interneuron genesis in the basal forebrain, we administered a short-pulse of BrdU to E13.5 embryos and compared the numbers of cycling medial ganglionic eminence (MGE) apical and basal progenitors in *LgDel* and WT embryos (Fig. 2*C*). We did not observe proliferative changes in MGE apical or basal progenitor pools. Apparently, the capacity of MGE-derived interneurons to move into the cerebral cortex in the *LgDel* 22q11.2DS mouse model is selectively compromised, as seen in single-gene mutations that disrupt interneuron migration.

We next asked whether this disruption of cortical interneuron progress is transient or sustained. The delay in tangential progress visible at E13.5 was not noticeable at either E14.5 or E15.5. At E14.5, however, there are significantly more interneurons in the ventricular zone (VZ) in the *LgDel* cortex (Fig. 2*D*), again resembling phenotypes seen in homozygous *Cxcr4* mutants (21, 27). At E15.5, interneurons have accumulated in the marginal zone (MZ) and have decreased in the subventricular zone (SVZ) stream (Fig. 2*E*). This dynamism in the distribution of migratory interneurons between the MZ, SVZ, and VZ streams in *LgDel* embryos parallels that reported for *Cxcr4*-homozygous mutants during this developmental epoch and prefigures altered distribution of interneurons in both genotypes. Apparently changes in interneuron migratory trajectories following 22q11.2 deletion resemble those associated with loss of function of genes that influence interneuron motility during midgestation.

To determine directly whether these defects reflect altered motility of nascent *LgDel* interneurons, we imaged interneurons as they migrate into the cortex in live slices from E13.5 *Dlx5/6*-CIE embryonic forebrains. Interneurons migrate tangentially into the *LgDel* cortex at a significantly reduced rate (Fig. 3 *A* and *B* and Movies S1 and S2), consistent with diminished progress of cortical interneurons through the cortical hemisphere (Fig. 2). *LgDel* interneurons also deviate from tangential routes. Significantly more *LgDel* interneurons move radially between MZ and SVZ migratory streams (Fig. 3 *C* and *D* and Movies S3 and S4), consistent with the redistribution of cells in the MZ and SVZ in the *LgDel* that accumulate by E15.5 (Fig. 2). Together, our data demonstrate aberrant position, motility, and migratory route selection of *LgDel* interneurons in the developing cortex. These changes are similar to those reported for interneuron motility in *Cxcr4*-homozygous mutants (25). Thus, diminished 22q11.2 gene dosage compromises cellular mechanisms of interneuron migration that also are the target of single genes that define regulatory pathways for the movement of these cells in developing cortex.

Cell-Autonomous Defects in *LgDel* Cortical Interneurons. We next asked whether the altered position, progress, and movement of *LgDel* interneurons reflect altered motility and migratory capacity of MGE-generated interneurons themselves. We dissected E12.5 MGE from *Dlx5/6*-CIE WT and *LgDel* embryos and grew these explants in a 3D collagen matrix. After 3 d, we compared the degree of dispersion of interneurons migrating from the MGE tissue mass. We observed a reduced area of cells dispersed from *LgDel* MGE explants (Fig. 4 *A*–C). This reduction was observed in a minimally enriched environment consisting of 3D collagen substrate and serum-free medium. Accordingly, it is likely that cell-autonomous disruption of the migratory capacity of MGE-derived cells contributes to altered movement of interneurons into the cortical rudiment during early development in *LgDel* mice.

Aberrant migration of nascent *LgDel* interneurons, either isolated in explants or observed in the developing cortex (Figs. 2 and 3), suggests significant changes in gene expression in these cells or in their migratory substrates because of diminished 22q11.2 gene dosage. Thus, we separated cortical substrate cells from *Dlx5/6*-CIE–labeled interneurons in microdissected E14.5 *LgDel* and WT cortex using fluorescence-activated cell sorting (FACS) (Fig. 4 *D*–*G*) and compared gene expression using Affymetrix microarrays (Tables S1 and S2). These changes then were confirmed by quantitative PCR (qPCR) in cDNAs as well as quantitative protein measurements in parallel samples of FACS-purified cells.

In *Dlx5/6*-CIE–negative cortical substrate cells, some altered transcripts could modify the interneurons' migratory environment. These alterations include the cell-adhesion molecule *Ephb1*, whose preferred ligand, *Ephrin-b1* is expressed at comparable levels in WT and *LgDel* migrating interneurons. Cellular stress genes also were altered, including *Metalliothionen2* (*Mt2*) (Fig. 4*H*), consistent with a previous report of elevated expression in cardiac primordia in the *Df1* 22q11.2DS model (31).

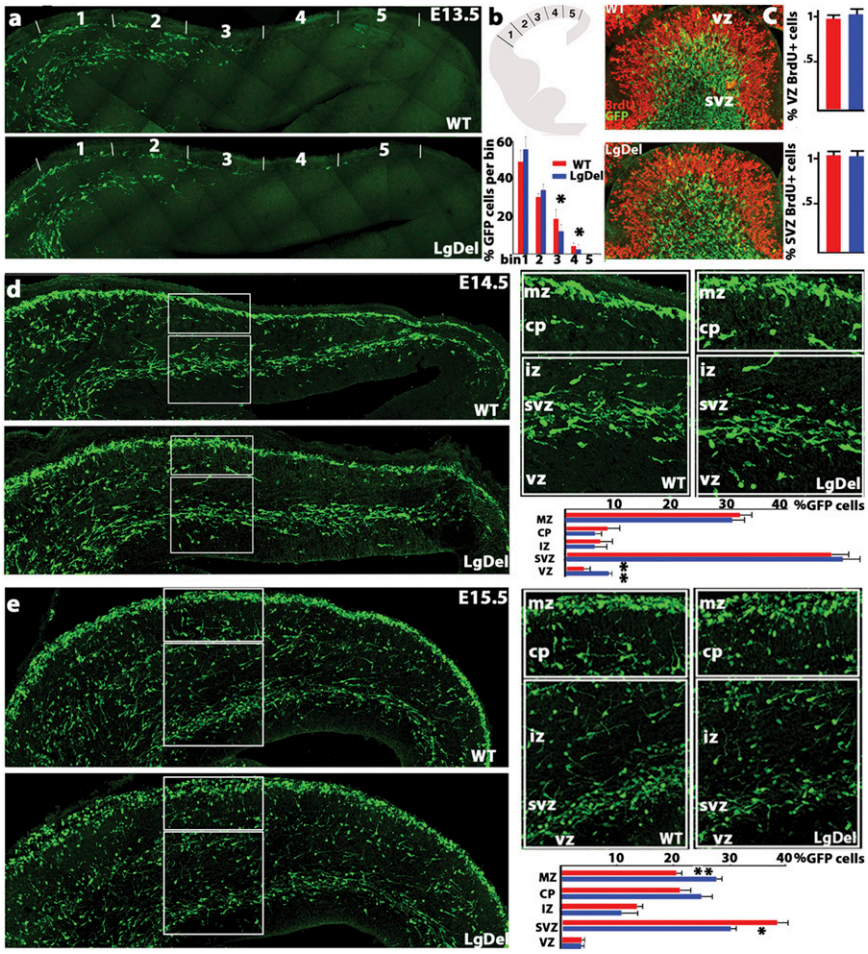

Fig. 2. Interneuron progress is disrupted in the embryonic *LgDel* cortex. *LgDel* embryonic cortical interneurons were labeled with GFP under the control of a *Dlx5/6* promoter element that limits expression to ventral forebrain-derived cells (*Dlx5/6*-CIE line). (*A*) E13.5 *LgDel* interneurons (*Lower*) are less frequent in the *LgDel* dorsal cortex. (*B*) Tangential interneuron migration measured in five equidistant bins between the cortical/subcortical boundary (bin 1) and the cortical hem (bin 5) is less advanced in the *LgDel* ($n = 5$ per genotype, ANOVA with subsequent bin comparison by LSD test, $*P \leq 0.048$ bin 3 and $*P = 0.04$ bin 4). (*C*) Images of E13.5 MGE showing *Dlx5/6*-CIE interneurons (green) and BrdU immunoreactivity (red). (BrdU was injected 45 min before animals were killed.). No significant proliferation differences were observed in apical (VZ; only BrdU single-labeled cells were counted) or basal (SVZ; only BrdU single-labeled cells were counted) MGE domains. $n = 5$ embryos per genotype; error bars represent SEM. (*D*) Cortical interneuron distribution between the ventricular and pial surfaces at E14.5 shows ectopic VZ interneurons ($n = 5$ per genotype, LSD test, $**P = 0.007$). *Insets* show MZ, CP, IZ, SVZ, and VZ. (*E*) The frequency of E15.5 *LgDel* migrating interneurons in the SVZ stream is reduced with a coincident increase in MZ stream cells ($n = 5$ per genotype, LSD test, $**P = 0.003$, $*P = 0.02$).

In the *Dlx5/6*-CIE–labeled interneuron population, expression levels of several genes that regulate interneuron migration and placement decline (Fig. 4*I*). These genes include *Cux2* and *Lhx6,* transcription factors previously shown to regulate interneuron migration and differentiation (26, 30, 32, 33). *Gad2* (*Gad65*), which encodes one of the key synthetic enzymes for the predominant cortical interneuron neurotransmitter GABA (34), is also diminished. Finally, expression of the chemokine receptor *Cxcr4*, which has a cell-autonomous role in guiding nascent interneurons in the cortex (23, 25), is decreased by ~35%. In contrast, expression of an additional cytokine receptor implicated in migration, *Cxcr7*, and the primary ligand for Cxcr4, *Cxcl12,* are not altered in *LgDel* interneurons or substrate cells. This observation raises the possibility that 22q11.2 interneuron migratory phenotypes might be the consequence of cell-autonomous changes in Cxcr4 expression and activity.

To establish whether Cxcr4 is indeed diminished in FACS-purified *Dlx5/6*-CIE interneurons, we measured total Cxcr4 protein and found a reduction comparable to the *Cxcr4* transcript (Fig. 4*J*). We also assessed phosphorylated Cxcr4, which was reduced by ~34% compared with WT FACS-purified interneurons (Fig. 4*J*). Disrupted interneuron migration may reflect decreased cell-surface Cxcr4 capable of transducing extracellular signals; however, Cxcr4 is present both at the interneuron surface and in cytoplasmic compartments (27). Accordingly, we compared the abundance of cell-surface Cxcr4 receptors on *LgDel* and WT interneurons using flow cytometry. We found a significant reduction in the immunolabeling intensity for Cxcr4 on the cell surface of *LgDel* interneurons (Fig. 4*K*). Thus, interneurons in *LgDel* embryos have a reduction of Cxcr4 protein on their surfaces as they migrate in the developing cerebral cortex. These changes provide a framework for evaluating whether specific molecular mechanisms for cell-autonomous disruption of interneuron migration resulting from diminished 22q11.2 gene dosage engage the same pathways as those that depend on Cxcr4 function.

Diminished Cxcr4 Dosage Modifies Distribution of Migrating *LgDel* Interneurons. Altered Cxcr4 expression and activity and the similarity of *LgDel* and *Cxcr4*$^{-/-}$ interneuron phenotypes (21–25) suggest that diminished 22q11.2 gene dosage and disrupted Cxcr4 signaling compromise similar aspects of interneuron migration, particularly the distribution of cells in the MZ, SVZ, and VZ migratory streams. If so, one would expect further diminished *Cxcr4* expression to modify distinct aspects of the *LgDel* interneuron phenotype selectively and proportionately.

We crossed *LgDel*:*Dlx5/6*-CIE mice with mice carrying one floxed *Cxcr4* allele (*Cxcr4*$^{wt/f}$) (35), resulting in heterozygous *Cxcr4* deletion in *Dlx5/6*-CIE cells (Fig. 5 *A*–*C*). We confirmed that this manipulation results in decreased Cxcr4 cell-surface labeling by FACS analysis (Fig. S2). Disrupted tangential interneuron migration into the cortical rudiment in the *LgDel* is not altered further by additionally reduced *Cxcr4* expression in E13.5 *LgDel*:*Dlx5/6*-CIE/*Cxcr4*$^{wt/f}$ embryos (Fig. 5*D*), in concert with observations in *Cxcr4*$^{-/-}$ at this stage (21). In contrast, the SVZ interneuron stream was altered in the *LgDel*:*Dlx5/6*-CIE/*Cxcr4*$^{wt/f}$ embryos, with substantially more interneurons displaced into the VZ, often displaying radially orientated processes (Fig. 5*E*), in accord with the ectopic distribution of interneurons in the VZ of E13.5 *Cxcr4*$^{-/-}$ embryos (21). Indeed, the severity of

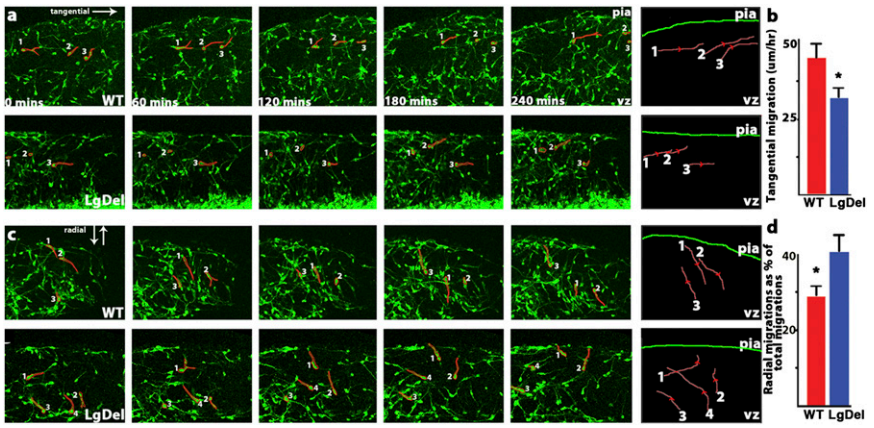

Fig. 3. Movement of embryonic interneurons is disrupted in the *LgDel*. (*A*) Time series of E13.5 live-imaged forebrain slices in which migrating interneurons (left to right) have been labeled genetically using the *Dlx5/6*-CIE transgene. (*Upper*) WT. (*Lower*) *LgDel*. The numerals and red outlines identify representative cells and their positions over the 4-h interval shown. (*Far Right*) Examples of migratory trajectories of individual cells imaged over 4 h. (*B*) Interneurons have a reduced velocity in the cortex relative to WT (n = 30 migratory neurons in five embryos per genotype, t test, $^*P = 0.032$). (*C*) Time series of embryonic interneurons in transition from tangentially to radially directed migration (left to right). (*Upper*) WT. (*Lower*) *LgDel*. The numbers and red outlines indicate the migratory state and direction for representative interneurons over the 4-h interval. (*Far Right*) Representative examples of radial migratory trajectories of individual cells imaged over 4 h. (*D*) Radial migrations occur more frequently in *LgDel* interneurons (five embryos per genotype, t test, $^*P = 0.039$).

the VZ/SVZ phenotype is graded and proportional so that *LgDel*:*Dlx5/6*-CIE/*Cxcr4*$^{wt/f}$ > *LgDel*:*Dlx5/6*-CIE > WT:*Dlx5/6*-CIE/*Cxcr4*$^{wt/f}$ (Fig. 5*E*) with approximate doubling observed between genotypes.

Thus, 22q11.2 deletion disrupts an established molecular mechanism for interneuron migration—Cxcr4-mediated signaling—resulting in strikingly similar changes in interneuron movement and distribution.

Discussion

Interneuron phenotypes in the *LgDel* mouse model of 22q11.2DS—a genetic syndrome associated with increased risk for cortical circuit disorders—are substantially similar to those caused by loss-of-function mutations in single genes that regulate parallel aspects of interneuron development. We established interneuron cell autonomy for these shared phenotypes and found cellular and molecular deficits specific to migration. Diminished 22q11.2 dosage reduces the expression of a number of genes with significant influence on interneuron migration, including *Cxcr4*. Interneuron-specific mutation of *Cxcr4* in the context of diminished 22q11.2 gene dosage selectively and proportionately enhances migratory phenotypes shared by 22q11.2-deleted *LgDel* and *Cxcr4*$^{-/-}$ mice. Accordingly, we suggest 22q11.2DS is in part a neuronal migration disorder in which diminished 22q11.2 gene dosage disrupts interneuron migration via a Cxcr4-dependent mechanism.

Diminished 22q11.2 gene dosage, like several single-gene mutations including *Lhx6*, *Cxcr7*, and *Cxcr4*, alters cortical circuitry by changing the placement and frequency of interneurons. Diminished 22q11.2 dosage selectively compromises a temporally distinct subset of parvalbumin interneurons most likely generated in the ventral MGE. Indeed, the migration and placement of calbindin (broad origin), calretinin [mainly caudal ganglionic eminence (36)], and somatostatin interneurons [dorsal MGE (37)] are not compromised in *LgDel* mice. The laminar redistribution of parvalbumin interneurons, without a reduction in frequency, likely reflects the disruption of two established migration mechanisms. First, additional MZ migratory interneurons result in increased upper-layer parvalbumin cells because of enhanced local radial ingression into layers 2/3 (28). Second, heterochronic, heterotopic VZ interneurons anomalously ascend radially to layers 2/3 rather than to layers 5/6. In 22q11.2DS, such changes may alter local inhibitory networks and oscillatory properties that depend upon parvalbumin interneuron integrity (20, 38, 39) and lead to cellular pathology parallel to that in the cortex of schizophrenic and autistic patients (8, 9).

There is significant cell autonomy and specificity for interneuron deficits caused by diminished 22q11.2 gene dosage. The transcriptional profile of cortical substrate cells yields few obvious candidates: genes for motogenic or chemotropic ligands and adhesion, trophic, and tropic molecules are not altered. In contrast, transcriptional differences in migratory interneurons include diminished expression of candidates known to influence interneuron genesis, migration, placement, and function: *Lhx6*, *Cux2, Gad2,* and, perhaps most compelling, the cytokine receptor gene *Cxcr4*. Accordingly, 22q11.2DS targets interneurons by disrupting a genetic network that regulates migration. Our results provide direct evidence that CNVs associated with cortical circuit disorders can modify cellular and molecular mechanisms essential for circuit development.

Reduced Cxcr4 expression in *LgDel* migrating interneurons—based upon mRNA and protein measurements—places cytokine regulation of interneuron migration via Cxcr4 (21-25) squarely in the context of cortical circuit disorder pathogenesis. There are several similarities between interneuron defects in *LgDel* and *Cxcr4*$^{-/-}$ embryos. In both instances, pallial migration is slowed and disordered, and ectopic interneurons are seen in the VZ (21, 22, 25). In utero pharmacological blockade of Cxcr4 in the MGE as well as transplantation of *Cxcr4*$^{-/-}$ MGE cells into WT embryos results in altered distribution of presumed parvalbumin interneurons in the postnatal cortex (22). Thus, reduced Cxcr4 in migratory interneurons emerges as a likely contributor to disrupted transit and final distribution of parvalbumin interneurons caused by diminished 22q11.2 gene dosage. In *LgDel* interneurons, altered transcriptional regulation via *Lhx6* and *Cux2* may diminish *Cxcr4* expression (30) in presumptive parvalbumin cells, whereas *Cxcr4* levels in other classes of cells approximate WT levels (21, 40). Our results therefore outline a network of interacting genes, with *Cxcr4* as a key node, perhaps modulated by *Lhx6* and *Cux2*, by which diminished 22q11.2 gene expression selectively disrupts interneuron development.

Our targeted genetic inactivation of one copy of *Cxcr4* in *LgDel* interneurons defines a molecular mechanism for 22q11.2 gene dosage-dependent regulation of interneuron migration. *LgDel* interneurons, with decreased surface Cxcr4, are relatively insensitive to cortical Cxcl12 signals. Reduced Cxcr4 signaling causes displacement of interneurons into the VZ. We suggest that this displacement may be followed by heterochronic migration into the cortex that terminates in layers 2/3, as is appropriate based on the time of arrival in the VZ, rather than in layers 5/6, as would be appropriate for the birthdates of these interneurons. Normally, at E13.5, cohorts of recently MGE-generated interneurons (41) enter the cortex via the SVZ stream (28). This population, delayed and misdirected as it enters the pallium, likely constitutes the ectopic migrating interneurons in the SVZ/VZ of E13.5 *LgDel* embryos. It is this subset of cells whose numbers likely are enhanced when

Cxcr4 cell-surface availability is diminished further in the *LgDel*:*Dlx5/6*-CIE/*Cxcr4*$^{wt/f}$ cortex. These Cxcr4-compromised cells eventually could account for misplaced parvalbumin neurons in the *LgDel* model of 22q11.2DS.

Neurodevelopmental hypotheses of schizophrenia and autism, the cortical circuit disorders most frequently associated with 22q11.2DS (42, 43), have suggested that pathogenesis results from disrupting cellular and molecular mechanisms for cortical development. Nevertheless, there was little evidence that specific mechanisms are compromised by diminished 22q11.2 gene expression or any other mutation associated with cortical circuit disorders. Our evidence shows that dosage changes can alter key regulatory pathways for cortical development in 22q11.2DS. It remains to be determined if other genetic syndromes associated with cortical circuit disorders similarly disengage established cellular and molecular mechanisms, resulting in aberrant cortical circuit formation.

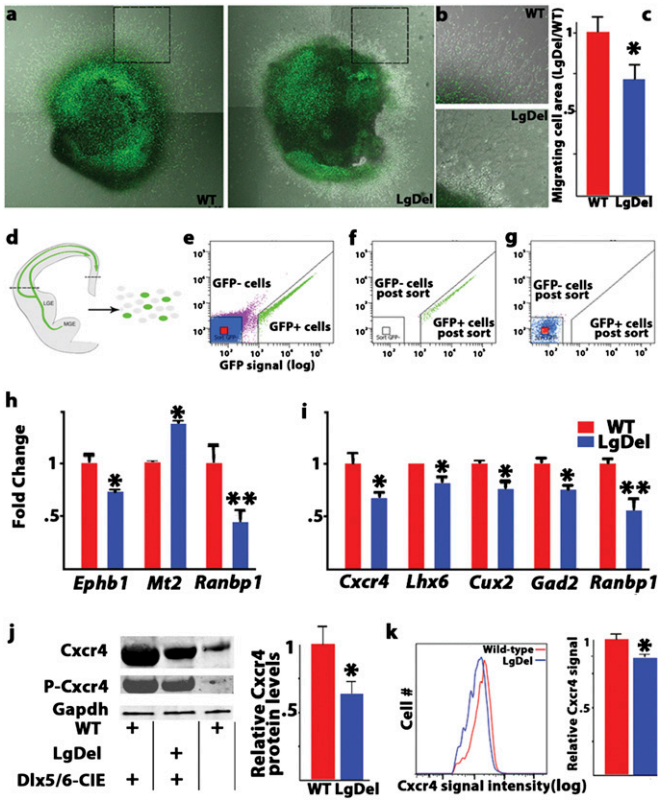

Fig. 4. Cell-autonomous defects in *LgDel* cortical interneurons. (*A*) Cell migration differs in explants of WT (*Left*) and *LgDel* (*Right*) Dlx5/6-CIE MGE. (*B*) Higher-magnification images show reduced migration from *LgDel*MGE explants. (*C*) There was a significant reduction in surface area covered by *LgDel* cells ($n = 8$ embryos per genotype, $^*P = 0.021$, *t* test). (*D*) Schematic of dissected tissue (dotted lines) collected for FACS analysis of migrating interneurons and their cortical substrate cells. (*E*) A representative FACS plot of *Dlx5/6*-CIE–labeled and –unlabeled cortical cells (green and red, respectively). (*F* and *G*) *Dlx5/6*-CIE–labeled (*F*) and –unlabeled (*G*) cortical cells were reanalyzed after FACS to verify sorting efficiency. (*H* and *I*) RT-qPCR confirmation of altered gene expression between WT and *LgDel Dlx5/6*-CIE–unlabeled cortical cells (*H*) and WT and *LgDel Dlx5/6*-CIE–labeled cortical interneurons (*I*) ($n = 3$ pooled samples per genotype, *t* test, $^*P \leq 0.05$, $^{**}P \leq 0.01$). (*J*) Western blot for Cxcr4 protein in *Dlx5/6*-CIE WT (*Left*) and *LgDel* (*Center*) interneurons isolated by FACS shows reduced total Cxcr4 protein in *LgDel* versus WT ($^*P = 0.039$, *t* test). Phosphorylated Cxcr4 (P-Cxcr4) was similarly reduced in *LgDel* samples. Both phosphorylated and total Cxcr4 protein levels are minimal in *Dlx5/6*-CIE–unlabeled cells (*Right*). (*K*) Representative flow cytometry histograms showing reduced signal for cell-surface Cxcr4 antibody labeling of E14.5 dissociated *LgDel Dlx5/6*-CIE cortical interneurons. The mean Cxcr4 cell-surface fluorescence in *LgDel Dlx5/6*-CIE$^+$ Cxcr4$^+$ cells was reduced relative to WT cells (*Right*) ($n = 10$ WT, 9 *LgDel* embryos; $^*P = 0.032$, *t* test).

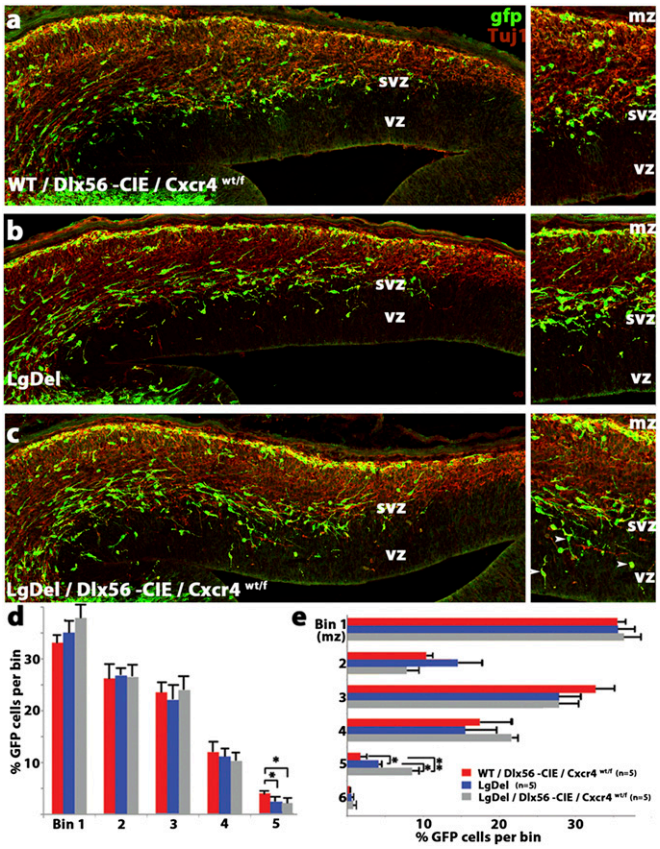

Fig. 5. Targeted heterozygous *Cxcr4* mutation selectively modifies interneuron migration in the developing *LgDel* cortex. There is a visible difference in the distribution of *Dlx5/6*-CIE interneurons in the VZ/SVZ of (*A*) E13.5 WT/*Dlx5/6*-CIE/Cxcr4$^{wt/f}$, (*B*) *LgDel*, and (*C*) *LgDel*/*Dlx5/6*-CIE/Cxcr4$^{wt/f}$ cortex. (*D*) Tangential interneuron progress into cortex was quantified between the cortical/subcortical boundary and the cortical hem. There was an equivalent, significant reduction of tangential migration in the *LgDel* and *LgDel*/*Dlx5/6*-CIE/Cxcr4$^{wt/f}$ embryos. (*E*) Interneuron distribution was quantified in six equidistant bins between the pial and ventricular surfaces. Migratory interneuron frequency in the VZ of the *LgDel* is increased relative to WT (WT/*Dlx5/6*-CIE/Cxcr4$^{wt/f}$; LSD test, $P = 0.045$ at bin location 5), and this altered frequency is increased further in the *LgDel*/*Dlx5/6-CIE*/Cxcr4$^{wt/f}$ (LSD test; $P = 0.003$ at bin location 5). Furthermore, there is a significant increase in interneurons in the VZ of the *LgDel*/*Dlx5/6-CIE*/Cxcr4$^{wt/f}$ over the *LgDel* (LSD test; $P = 0.05$; error bars represent SEM).

Materials and Methods

Mice. Animal experimental procedures were approved by The George Washington University institutional animal care and use committee. The *Dlx5/6*-CIE (29), *Cxcr4* $^{f/f}$ (35), and *LgDel* (10) lines were kept on a C57/BL6 background.

Real-Time Imaging. Forebrain slices (250 μm) prepared on a vibratome from E13.5 brains were placed on nucleopore membrane filters (Whatman) over 35-mm imaging dishes containing slice culture medium (44). Slices were transferred to a 37 °C/5% CO_2 chamber and visualized with an Olympus FV1000 confocal microscope. Slices were imaged every 6 min for 12 h. Migration was quantified using Imaris software (Bitplane).

Quantitative and Statistical Analysis. To determine interneuron distribution at postnatal day (P)21, a counting box subdivided into six equidistant bins that spanned the pial surface-to-white matter tract was placed systematically in cortical locations at the level of the anterior commissure (area 6 of the mouse frontal association cortex). At E13.5, cells were counted in five equidistant bins

between the cortical/subcortical boundary and the cortical hem. At E14.5 and E15.5, interneuron distribution between the pial and ventricular surfaces was determined for cytologically distinct zones [MZ, cortical plate (CP), intermediate zone (IZ), SVZ, and VZ] within a single counting box. Two independent observers, blinded to genotype, counted cells from the immunolabeled material. The data were analyzed using Student *t* test, ANOVA, and post hoc Fisher's least significant difference test (LSD) (Graphpad, Inc.).

Tissue Dissociation and FACS. Embryonic cortices were dissociated in papain (Worthington Biochemical). FACS then was performed on a FACSAria flow cytometer (BD Biosciences). Cells were gated using forward and orthogonal light scatter, and GFP fluorescence was captured in the detector with a 530/30 bandpass filter. After collection, cells were lysed in TRIzol for RNA isolation (Invitrogen). For Cxcr4 cell-surface labeling, an Alexa Fluor 647-nm–conjugated rat anti-Cxcr4 antibody (BioLegend) was added to dissociated embryonic cortical cells and measured by flow cytometry using a HeNe laser (633-nm excitation). Analysis was conducted using FlowJo software (Tree Star,Inc.).

Microarray and RT-qPCR. RNA was extracted from TRIzol samples and purified using RNeasy spin columns (Qiagen). For cRNA synthesis and array hybridization, 100 ng of total RNA was used. Samples were hybridized to the mouse gene 1.0 ST array (Affymetrix). cDNA synthesis reactions were conducted as previously described (18). qPCR was conducted on a CFX384 thermal cycler using EvaGreen reagent (BioRad). Primer sequences used are listed in Table S3.

Immunohistochemistry. Fixed embryonic and postnatal brains were processed and stained as described previously (18). Primary antibodies used are listed in Table S4. Species-specific fluorescently conjugated secondary antibodies (Invitrogen) were applied subsequently.

Nucleotide Analog Injections. Timed pregnant mice (E13.5 for proliferation and E13.5/E15.5, for birth-dating) were injected i.p. with BrdU (50 mg/kg body weight) and iododeoxyuridine (IdU; 70 mg/kg). Standard BrdU/IdU immunolabeling techniques were used after antigen retrieval by steam treatment in sodium citrate buffer.

Explant Assay. E12.5 MGE explants were grown in collagen matrix for 72 h at 37 °C/5% CO_2 in neurobasal medium supplemented with B27 and L-glutamine (Invitrogen). Collagen (Rat Tail Collagen I; BD Biosciences) was prepared by NaHCO3 neutralization and diluted 1:3 before plating.

Western Blot. FACS samples were resolved using 4–12% SDS–PAGE and were transferred electrophoretically onto PVDF membrane (Amersham Biosciences). The membrane was incubated in primary antibody for 1 h at room temperature and then with species-appropriate fluorescently conjugated secondary antibody (Licor). Each sample was probed with a rabbit anti-Cxcr4 antibody (Abcam) or rabbit anti-phospho Cxcr4 antibody (Ecm Biosciences) and normalized to Gapdh. Fluorescence was measured on a Licor Odyssey-system.

ACKNOWLEDGMENTS. We thank Thomas Harrigan for technical support. We thank Teresa Hawley for FACS analysis. This work was supported by National Institutes of Health (NIH)National Institute of Child Health and Human Development Grant 042182 and NIH/National Institute of Mental Health Grant 64065 (to A-S.L.), Grant S10RR025565 for microscopic analysis, and National Institute of Neurological Disorders and Stroke Grant NS031768 for the University of North Carolina at Chapel Hill Neuroscience Center core facility. D.W.M. was funded by a National Alliance for Research on Schizophrenia and Depression Young Investigator Award from the Brain and Behavior Research Foundation.

1. Rubenstein JL, Merzenich MM (2003) Model of autism: Increased ratio of excitation/inhibition in key neural systems. *Genes Brain Behav* 2(5):255–267.
2. Rippon G, Brock J, Brown C, Boucher J (2007) Disordered connectivity in the autistic brain: Challenges for the "new psychophysiology". *Int J Psychophysiol* 63(2):164–172.
3. Insel TR (2010) Rethinking schizophrenia. *Nature* 468(7321):187–193.
4. Fishell G, Rudy B (2011) Mechanisms of inhibition within the telencephalon: "Where the wild things are". *Annu Rev Neurosci* 34:535–567.
5. Benes FM (2000) Emerging principles of altered neural circuitry in schizophrenia. *Brain Res Brain Res Rev* 31(2-3):251–269.
6. Lewis DA, Hashimoto T, Volk DW (2005) Cortical inhibitory neurons and schizophrenia. *Nat Rev Neurosci* 6(4):312–324.
7. Blatt GJ, Fatemi SH (2011) Alterations in GABAergic biomarkers in the autism brain: Research findings and clinical implications. *Anat Rec (Hoboken)* 294(10):1646–1652.
8. Beasley CL, Zhang ZJ, Patten I, Reynolds GP (2002) Selective deficits in prefrontal cortical GABAergic neurons in schizophrenia defined by the presence of calcium-binding proteins. *Biol Psychiatry* 52(7):708–715.
9. Hashimoto T, et al. (2003) Gene expression deficits in a subclass of GABA neurons in the prefrontal cortex of subjects with schizophrenia. *J Neurosci* 23(15):6315–6326.
10. Merscher S, et al. (2001) TBX1 is responsible for cardiovascular defects in velo-cardio-facial/DiGeorge syndrome. *Cell* 104(4):619–629.
11. Murphy KC, Jones LA, Owen MJ (1999) High rates of schizophrenia in adults with velo-cardio-facial syndrome. *Arch Gen Psychiatry* 56(10):940–945.
12. Niklasson L, Rasmussen P, Oskarsdottir S, Gillberg C (2009) Autism, ADHD, mental retardation and behavior problems in 100 individuals with 22q11 deletion syndrome. *Res Dev Disabil* 30(4):763–773.
13. Fine SE, et al. (2005) Autism spectrum disorders and symptoms in children with molecularly confirmed 22q11.2 deletion syndrome. *J Autism Dev Disord* 35(4):461–470.
14. Kiehl TR, Chow EW, Mikulis DJ, George SR, Bassett AS (2009) Neuropathologic features in adults with 22q11.2 deletion syndrome. *Cereb Cortex* 19(1):153–164.
15. Schaer M, et al. (2006) Abnormal patterns of cortical gyrification in velo-cardio-facial syndrome (deletion 22q11.2): An MRI study. *Psychiatry Res* 146(1):1–11.
16. van Amelsvoort T, et al. (2004) Brain anatomy in adults with velocardiofacial syndrome with and without schizophrenia: Preliminary results of a structural magnetic resonance imaging study. *Arch Gen Psychiatry* 61(11):1085–1096.
17. Mori T, et al. (2011) Neuroradiological and neurofunctional examinations for patients with 22q11.2 deletion. *Neuropediatrics* 42(6):215–221.
18. Meechan DW, Tucker ES, Maynard TM, LaMantia AS (2009) Diminished dosage of 22q11 genes disrupts neurogenesis and cortical development in a mouse model of 22q11 deletion/DiGeorge syndrome. *Proc Natl Acad Sci USA* 106(38):16434–16445.
19. Long JM, et al. (2006) Behavior of mice with mutations in the conserved region deleted in velocardiofacial/DiGeorge syndrome. *Neurogenetics* 7(4):247–257.
20. Sigurdsson T, Stark KL, Karayiorgou M, Gogos JA, Gordon JA (2010) Impaired hippocampal-prefrontal synchrony in a genetic mouse model of schizophrenia. *Nature* 464(7289):763–767.
21. Li G, et al. (2008) Regional distribution of cortical interneurons and development of inhibitory tone are regulated by Cxcl12/Cxcr4 signaling. *J Neurosci* 28(5):1085–1098.
22. López-Bendito G, et al. (2008) Chemokine signaling controls intracortical migration and final distribution of GABAergic interneurons. *J Neurosci* 28(7):1613–1624.
23. Stumm RK, et al. (2003) CXCR4 regulates interneuron migration in the developing neocortex. *J Neurosci* 23(12):5123–5130.
24. Tiveron MC, Cremer H (2008) CXCL12/CXCR4 signalling in neuronal cell migration. *Curr Opin Neurobiol* 18(3):237–244.
25. Wang Y, et al. (2011) CXCR4 and CXCR7 have distinct functions in regulating interneuron migration. *Neuron* 69(1):61–76.
26. Liodis P, et al. (2007) Lhx6 activity is required for the normal migration and specification of cortical interneuron subtypes. *J Neurosci* 27(12):3078–3089.
27. Sánchez-Alcañiz JA, et al. (2011) Cxcr7 controls neuronal migration by regulating chemokine responsiveness. *Neuron* 69(1):77–90.
28. Miyoshi G, Fishell G (2011) GABAergic interneuron lineages selectively sort into specific cortical layers during early postnatal development. *Cereb Cortex* 21(4):845–852.
29. Stenman J, Toresson H, Campbell K (2003) Identification of two distinct progenitor populations in the lateral ganglionic eminence: Implications for striatal and olfactory bulb neurogenesis. *J Neurosci* 23(1):167–174.
30. Zhao Y, et al. (2008) Distinct molecular pathways for development of telencephalic interneuron subtypes revealed through analysis of Lhx6 mutants. *J Comp Neurol* 510 (1):79–99.
31. Prescott K, et al. (2005) Microarray analysis of the Df1 mouse model of the 22q11 deletion syndrome. *Hum Genet* 116(6):486–496.
32. Cobos I, Long JE, Thwin MT, Rubenstein JL (2006) Cellular patterns of transcription factor expression in developing cortical interneurons. *Cereb Cortex* 16(Suppl 1): i82–i88.
33. Cubelos B, et al. (2008) Cux-1 and Cux-2 control the development of Reelin expressing cortical interneurons. *Dev Neurobiol* 68(7):917–925.
34. Erlander MG, Tillakaratne NJ, Feldblum S, Patel N, Tobin AJ (1991) Two genes encode distinct glutamate decarboxylases. *Neuron* 7(1):91–100.
35. Nie Y, et al. (2004) The role of CXCR4 in maintaining peripheral B cell compartments and humoral immunity. *J Exp Med* 200(9):1145–1156.
36. Xu Q, Cobos I, De La Cruz E, Rubenstein JL, Anderson SA (2004) Origins of cortical interneuron subtypes. *J Neurosci* 24(11):2612–2622.
37. Wonders CP, et al. (2008) A spatial bias for the origins of interneuron subgroups within the medial ganglionic eminence. *Dev Biol* 314(1):127–136.
38. Hensch TK (2005) Critical period plasticity in local cortical circuits. *Nat Rev Neurosci* 6 (11):877–888.
39. Sohal VS, Zhang F, Yizhar O, Deisseroth K (2009) Parvalbumin neurons and gamma rhythms enhance cortical circuit performance. *Nature* 459(7247):698–702.
40. Tanaka DH, et al. (2010) CXCR4 is required for proper regional and laminar distribution of cortical somatostatin-, calretinin-, and neuropeptide Y-expressing GABAergic interneurons. *Cereb Cortex* 20(12):2810–2817.
41. Rubin AN, et al. (2010) The germinal zones of the basal ganglia but not the septum generate GABAergic interneurons for the cortex. *J Neurosci* 30(36):12050–12062.
42. Geschwind DH, Levitt P (2007) Autism spectrum disorders: Developmental disconnection syndromes. *Curr Opin Neurobiol* 17(1):103–111.
43. Weinberger DR (1987) Implications of normal brain development for the pathogenesis of schizophrenia. *Arch Gen Psychiatry* 44(7):660–669.
44. Polleux F, Ghosh A (2002) The slice overlay assay: A versatile tool to study the influence of extracellular signals on neuronal development. *Sci STKE* 2002(136):pl9.